Heliyon 6 (2020) e04136

Contents lists available at ScienceDirect

Heliyon

journal homepage: www.cell.com/heliyon

Research article

A comparative energy and exergy optimization of a supercritical-CO_2 Brayton cycle and Organic Rankine Cycle combined system using swarm intelligence algorithms

Guillermo Valencia Ochoa [a,*], Jorge Duarte Forero [a], Jhan Piero Rojas [b]

[a] Programa de Ingeniería Mecánica, Universidad del Atlántico, Carrera 30 Número 8-49, Puerto Colombia, Barranquilla 080007, Colombia
[b] Engineering Faculty, Universidad Francisco de Paula Santander, Avenida Gran Colombia No. 12E-96, Cúcuta 540003, Colombia

ARTICLE INFO

Keywords:
Energy
Mechanical engineering
Thermodynamics
Mathematical optimization
Energy conservation
Swarm intelligence algorithms
Brayton supercritical CO_2 cycle
Organic Rankine cycle
Exergetic analysis
Energy analysis

ABSTRACT

This article presents a multivariable optimization of the energy and exergetic performance of a power generation system, which is integrated by a supercritical Brayton Cycle using carbon dioxide, and a Simple Organic Rankine Cycle (SORC) using toluene, with reheater ($S-CO_2^{RH}-SORC$), and without reheater ($S-CO_2^{NRH}-SORC$) using the PSO algorithm. A thermodynamic model of the integrated system was developed from the application of mass, energy and exergy balances to each component, which allowed the calculation of the exergy destroyed a fraction of each equipment, the power generated, the thermal and exergetic efficiency of the system. In addition, through a sensitivity analysis, the effect of the main operational and design variables on thermal efficiency and total exergy destroyed was studied, which were the objective functions selected in the proposed optimization. The results show that the greatest exergy destruction occurs at the thermal source, with a value of 97 kW for the system without Reheater (NRH), but this is reduced by 92.28% for the system with Reheater (RH). In addition, by optimizing the integrated cycle for a particle number of 25, the maximum thermal efficiency of 55.53% (NRH) was achieved, and 56.95% in the RH system. Likewise, for a particle number of 15 and 20 in the PSO algorithm, exergy destruction was minimized to 60.72 kW (NRH) and 112.06 kW (RH), respectively. Comparative analyses of some swarm intelligence optimization algorithms were conducted for the integrated S-CO_2-SORC system, evaluating performance indicators, where the PSO optimization algorithm was favorable in the analyses, guaranteeing that it is the ideal algorithm to solve this case study.

1. Introduction

The promoting of environmental protection and energy efficiency has been the goal of increasing the thermal performance of the power generation processes [1], in addition to implementing renewable energy source combinations [2], and conventional source [3]. The use of waste heat recovery systems from various energy sources for generation purposes has continuously presented both technical and economic challenges, linked to the high purchase cost and low thermal efficiency of these solutions [4]. Therefore, it has been determined that the organic Rankine cycle (ORC) is very suitable for absorbing and recovering medium and low-quality waste heat [5, 6], and can be implemented in power conversion plants [7], increasing the efficiency of the primary system with the aim of developing more efficient processes for energy production [8].

Carbon dioxide has been widely used as a working fluid in thermal generation systems, due to its easy acquisition, relatively low economic cost, and its ability to withstand extremely high temperatures [9]. These characteristics have allowed the development of some researchers, such as Garg et al. [10] who carried out a comparative study between the different trans-critical, supercritical and subcritical systems with CO_2 as working fluid in a Brayton cycle, obtaining better results for the supercritical CO_2 system (S-CO_2) because it makes better use of the thermal properties of the fluid due to its operation near the critical point.

This phenomenon is related to the pre-compression in the Brayton S-CO_2 cycle, which implies high efficiency, higher heat transport capacity, and smaller equipment with lower acquisition costs [11]. Due to several studies related to the performance of the Brayton S-CO_2 cycle, it is observed that due to the use of smaller components, it has been possible to reduce the costs of energy generation [12]. The high-efficiency

* Corresponding author.
E-mail address: guillermoevalencia@mail.uniatlantico.edu.co (G. Valencia Ochoa).

https://doi.org/10.1016/j.heliyon.2020.e04136
Received 18 March 2020; Received in revised form 16 May 2020; Accepted 1 June 2020

capacity that can be achieved by the Brayton cycle is due to the reduction of compressor energy, which is reflected by significantly increasing the density of the supercritical fluid since increasing the density to a value close to the critical point reduces the energy consumption of the compressor [13]. Likewise, thermodynamically a great advantage of the Brayton carbon dioxide cycle consists of the high ratio of useful work to expansion, that is, lower energy to compression than the energy to expansion handling a range from 0.7 to 0.85 when the compressor input is at supercritical conditions [14].

On the other hand, Chacartegui et al. [15] proposed a different alternative for obtaining energy through a combined cycle that uses a gas turbine with carbon dioxide as the working fluid, and an Organic Rankine Cycle, obtaining promising results for integration with solar tower power plants. Also, Bae and lee [16] worked with a Brayton S-CO_2 hybrid system with the Organic Rankine Cycle, which improved the net performance of the system and the operating range taking into account that a lower volume of the recuperator can be used in the Brayton Cycle. Therefore, the ORC Cycle is considered a system that significantly increases the overall efficiency because it has the advantage of operating as a tail cycle and recovering heat from other alternative sources, such as heat rejection from other cycles, and engine exhaust gases, which require the use of a thermal oil that receives heat below its critical temperature and an organic fluid that adapts to the system [17].

Waste heat recovery systems based on ORC have become in recent years a technology that can be applied in energy conversion at an industrial level with great technical feasibility [18], and a good cost-benefit ratio [19]. ORC uses an organic fluid such as refrigerants and hydrocarbons, which fit into the system better than water to reduce heat source temperatures [20]. However, due to high pollution rates, environmental protection has been chosen, and fluids such as chlorofluorocarbons, which have a negative impact on the atmosphere, have been penalized in these applications [21], which makes the correct selection of the organic working fluid a great technical and research challenge [22].

Thus, Toffolo et al. [23] have oriented its research towards the economic profitability that can be obtained through the selection of an organic working fluid, and the adjustment of the operational parameters in the ORC system to obtain the best cycle configuration, based on a thermodynamic optimization procedure of the original system configuration, and design parameters that examine all possible configurations, design options around the best values of the objective function, and economic modeling procedure validated on real cost data, and the study of out-of-design behavior.

On the other hand, Zare V [24]. complemented with economic criteria, the thermal performance studies carried out on different ORC configurations, where the better energy results were obtained for the regenerative organic Rankine cycle. The economic analysis was carried out under a methodology that allowed the design of a profitable waste heat recovery system in terms of total investment capital, and operation and maintenance costs. However, in the event that equipment costs are not known, but technical details are available, they can be estimated using the percentage correlations of the equipment cost. Bejan et al. [25], Smith [26], and Towler [27] propose a correlation to calculate the costs for various types of process equipment.

To increase the performance of the ORC system, technical and economic criteria have been proposed for the optimal selection of the organic working fluid, taking into account the international standards and regulatory framework for the environmental preservation [28]. Similarly, one of the techniques used to increase the thermal performance of the system is to identify the components with the greatest irreversibilities through traditional exergetic analysis to propose improvement opportunities. However, this analysis does not provide the values of the operational and design variables that optimize system performance [29]. Thus, the implementation of optimization algorithms based on system models, in these cases, allows obtaining the optimal conditions to achieve the best performance and opportunities for energy and exergetic improvement, providing data on the portion of exergy destruction that can be avoided [30].

The development of new technologies has been considered among the main alternatives and techniques for increasing energy efficiency since they allow the modernization of machines and configurations of production systems by others that have a better overall efficiency [31, 32]. Increased overall efficiency in power generation systems such as supercritical Brayton cycles CO_2, can be effectively achieved by taking advantage of waste heat through an ORC, and optimizing it from an energetic and exergetic approach, this being the fundamental purpose of this work. There are several reasons why this work is being developed, among which the need to conserve natural resources, the limitations associated with the availability of spaces to generate energy in the places where these generation systems are installed, the cost savings required to make these solutions viable, the incentives obtained by proposing more efficient energy generation processes that have already been included in the energy policies, and regulatory framework in different countries [31].

Therefore, the main contribution of this article is to propose a comparative energy and exergy optimization using three swarm intelligence algorithms on the supercritical Brayton CO_2 system with and without reheating integrated to an ORC cycle as bottoming cycle, which allows to increase overall thermal efficiency and obtain viable energy generation indicator, aspects that currently limit its technological growth, acceptance, and dissemination of this technology in the industrial sector. The performance of the PSO, GA, and RPS algorithms is studied under two optimization problems in the combined Brayton-ORC thermal system, the exergy destruction minimization, and the thermal efficiency maximization using the elapsed time, the root mean square error and the diversity as performance indicators. Also, a two-sample z-test was conducted to determine the significance level of the swarm intelligence algorithms in the energy and exergy optimization of the thermal system.

2. Methodology

2.1. System description

Initially, the carbon dioxide at a high temperature and pressure point (St.1) enters the primary turbine (10) of the Brayton S-CO_2 cycle, and then it is reheated (13) and expanded at a lower pressure and temperature in the second turbine (11). Afterward, a recuperator is used to allow the reheating of the current that leaves the compressor (8) at point (St.7) and is directed to the heater (12) at point (St.8), while the St.5 current is cooled by yielding heat to the thermal oil so that it is subsequently compressed (St.6) by the compressor (8).

The thermal oil (Therminol 75) receives the heat in the heat exchanger (1), to be transferred to the SORC evaporator (2), which has three stages called preheating, evaporation and overheating, whose purpose is to transfer the heat to the toluene, and then through Pump 1 (3) drive the Therminol 75 to repeat the thermal oil circuit. Afterward, the organic fluid at a high temperature and pressure (St.12) enters the turbine (4) and is expanded by decreasing its pressure and temperature to enter the cooler (5) and the condenser (6), where the organic fluid is cooled by the water that enters at ambient pressure (St.17 - St.19), and then it is directed to the reservoir. Then, the working fluid when leaving the condenser (6) at point (St.15) is a saturated liquid, to enter Pump 2 (7), and then the evaporator (St.16), completing the cycle as shown in Figure 1.

2.2. Thermodynamic model

For the thermodynamic study of the system, the mass balance as shown in Eq. (1) is applied, and energy by means of Eq. (2) to each of the components considering a steady-state operation for the components, according to the thermophysical properties of the working fluids operating in the system. In the case of the Brayton S-CO_2 cycle, the carbon

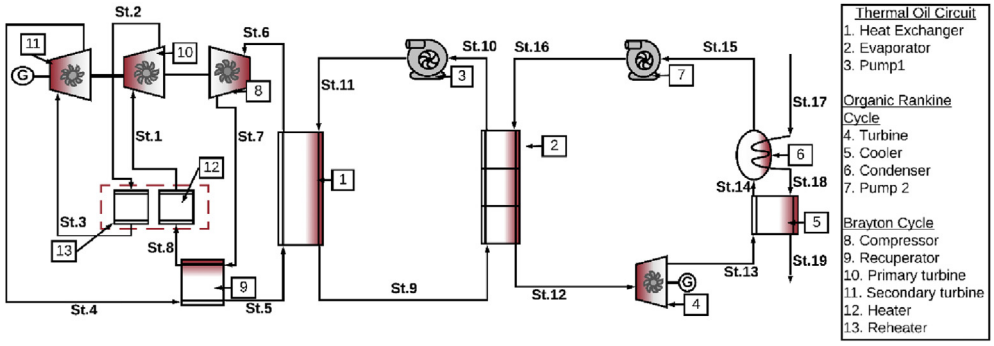

Figure 1. Graphic description of the Brayton S-CO_2- SORC power generation cycle.

dioxide approaches the critical point [33], while in the SORC the Toluene, has shown good performance in these systems [34], is considered as the organic working fluid.

$$\sum \dot{m}_{in} - \sum \dot{m}_{out} = 0 \tag{1}$$

$$\sum \dot{m}_{in} h_{in} - \sum \dot{m}_{out} h_{out} + \sum \dot{Q} + \sum \dot{W} = 0 \tag{2}$$

where $\dot{m}$ is the mass flow, h is the specific enthalpy of the fluid, $\dot{Q}$ and $\dot{W}$ are the heat and power rates, respectively. On the other hand, the net power of the Brayton cycle ($\dot{W}_{net,\ \text{Brayton S–CO2}}$), is calculated from the power values of the turbine primary (10) and secondary (11), and the compressor (8), as shown in Eq. (3), while the net power of the SORC in Eq. (4), is a function of the generated power of the turbine (4), Pump 1 (3), and Pump 2 (7).

$$\dot{W}_{net,\ \text{Brayton S–CO2}} = \dot{W}_{Primary\ turbine} + \dot{W}_{Secundary\ turbine} - \dot{W}_{Compressor} \tag{3}$$

$$\dot{W}_{net,\ SORC} = \dot{W}_{Turbine} - \dot{W}_{Pump\ 1} - \dot{W}_{Pump\ 2} \tag{4}$$

The specific physical exergy (e_{ex}) without considering the variation of kinetic and potential energy, was calculated by Eq. (5).

$$e_{ex} = (h_i - h_0) - T_0 \cdot (s_i - s_0) \tag{5}$$

where h_0 and s_0 correspond to the specific enthalpy and entropy at the reference conditions of temperature (T_0), and pressure (P_0), respectively. These reference conditions are $T_0 = 298.15\ \mathbf{K}$, and $P_0 = 101.325\ \mathbf{kPa}$.

For the exergetic analysis of the system, the balance of exergy was applied to each component of the system by means of the second law of thermodynamics (Equation 6) [35].

$$\dot{E}_d = \sum_{in}^{n} \dot{m} \cdot e_{ex} - \sum_{out}^{n} \dot{m} \cdot e_{ex} - \dot{E}_{\text{in}} - \dot{E}_{\text{out}} = T_0 \cdot \dot{S}_{gen} \tag{6}$$

where $\dot{E}_d$ is the destruction of exergy, $\dot{e}_{ex}$ is the exergy of flow, $\dot{E}_{\text{in}}$ and $\dot{E}_{\text{out}}$ out are the exergy by transfer of energy in the form of heat and work, and $\dot{S}_{gen}$ is the entropy generated.

From the results of the exergy balance, the exergetic efficiency was calculated (η_{ex}), both for the system and for each component of the thermal system is shown in Eq. (7).

$$\eta_{ex} = \frac{\dot{E}_{Product}}{\dot{E}_{Fuel}} \tag{7}$$

where $\dot{E}_{Fuel}$ is the exergy supplied to the component, while $\dot{E}_{Product}$ is the output exergy. The definition of Fuel-Product for each component of the system is shown in Table 1.

The thermal efficiency of the Brayton cycle ($\eta_{I,\ \text{Brayton S–CO2}}$) is calculated by Eq. (6), which is a function of the net power of the Brayton cycle, and the sum of the heat from the heater (12) and reheater (13), which make up the heat source.

$$\eta_{I,\ \text{Brayton S–CO2}} = \frac{\dot{W}_{net,\ \text{Brayton S–CO2}}}{\dot{Q}_{Heater} + \dot{Q}_{Reheater}} \tag{8}$$

Eq. (9) is used to calculate the thermal efficiency of the SORC cycle ($\eta_{I,\ SORC}$), the net power of the SORC cycle is taken into account, with respect to the heat recovered from the heat exchanger (1).

$$\eta_{I,\ SORC} = \frac{\dot{W}_{net,\ SORC}}{\dot{Q}_{heat\ exchanger}} \tag{9}$$

Thus, the overall efficiency of integrated system Brayton S-CO_2 – SORC is a function of net power and heat source, as shown in Eq. (10). Therefore, the integrated system presents an enhancement in the thermal efficiency respect to the Brayton cycle ($\Delta\eta_{ther}$).

$$\eta_{th,overall} = \frac{\dot{W}_{net,\ Brayton\ S–CO2} + \dot{W}_{net,\ SORC}}{\dot{Q}_{Heater} + \dot{Q}_{Reheater}} \tag{10}$$

Table 1. Fuel-Product definition for each component.

SORC				Brayton S-CO_2			
Component	Fuel	Product	Loss	Component	Fuel	Product	Loss
Heat exchanger	$\dot{E}_5$	$\dot{E}_9$-$\dot{E}_{11}$	$\dot{E}_{11}$	Compressor	$\dot{W}_{comp}$	$\dot{E}_7 - \dot{E}_6$	-
Pump1	$\dot{W}_{P1}$	$\dot{E}_{11}$-$\dot{E}_{10}$	-	Turbine primary	$\dot{E}_1 - \dot{E}_2$	W_{t1}	-
Evaporator	$\dot{E}_9$-$\dot{E}_{10}$	$\dot{E}_{12}$-$\dot{E}_{15}$	-	Turbine secondary	$\dot{E}_3 - \dot{E}_4$	W_{t2}	-
Turbine	$\dot{E}_{12}$-$\dot{E}_{13}$	$\dot{W}_{T1}$	-	Reheater and heater	$\dot{E}_8 - \dot{E}_1 + \dot{Q}_s$	$\dot{E}_3 - \dot{E}_2$	-
Cooler and condenser	-	-	$\dot{E}_{19}$	-	-	-	-
Pump2	$\dot{W}_{P2}$	$\dot{E}_{16}$-$\dot{E}_{15}$	-	Recuperator	$\dot{E}_4 - \dot{E}_5$	$\dot{E}_8 - \dot{E}_7$	-

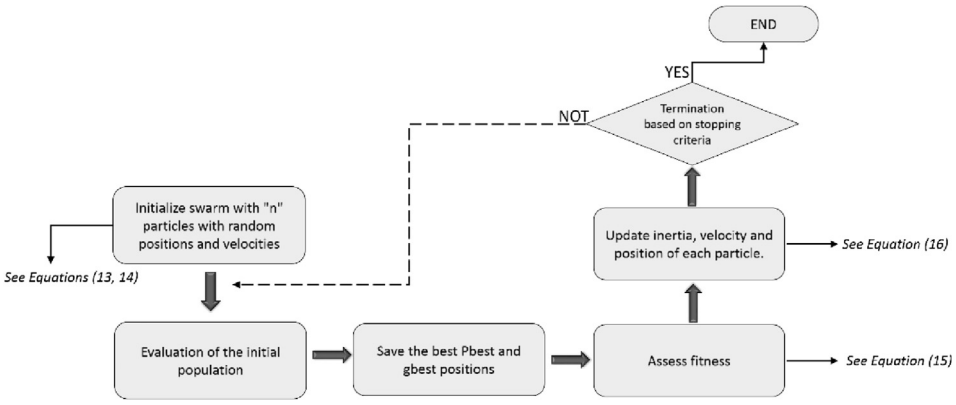

Figure 2. Flowchart of the PSO algorithm.

2.3. Optimization algorithms

Genetic algorithms consist of optimization methods developed to solve complex problems with many elements and a variety of constraints and variables coexisting in one or several solutions, which are not possible to approximate by means of linear programming. The methods to be used in this work are described in the following sections.

2.3.1. Particle swarm optimization (PSO)

It is a stochastic method of optimization, which addresses the behavior in the society of some communities of organisms such as swarms of insects, birds, groups of fish, among others. Therefore, such behavior is based on the transfer of events from each individual to others of the same group [36, 37] in which the movement of these to a more favorable position in specific search space is observed. In this way, this analogy previously commented is implemented where an algorithm based on a set or population of individuals called swarm was implemented, in which each individual called particle represents the possible solution. The flowchart of the PSO algorithm is shown in Figure 2, where it was implemented and developed in the software Matlab®.

The algorithm is made up of a swarm of i particles with negligible mass and volume, which move in the space of D dimensions. Therefore, the velocity vector that directs its movement from one position to another represents the capacity of the particle to find the solution.

The PSO model relates two types of learning for each particle. The first type is related to the personal experience that the particle develops as it moves through the search space and this behavior is defined as the position that gives the best value of the objective function taking into account the positions previously visited by the particle, it is presented as a vector and is known as *pbest*, which is described as follows.

$$\boldsymbol{\Psi_P} = \{\boldsymbol{\Psi_{P1}},\ \boldsymbol{\Psi_{P2}}, \ldots, \boldsymbol{\Psi_{PD}}\} \tag{11}$$

Likewise, the second type of learning is distinguished as *gbest* which is defined as the learning relationship that the particle obtains in relation to the interaction between it and the environment, in other words, it can be said that it is called a collective behavior is denoted vectorially as shown below in Eq. (12) [37].

$$\psi_g = \{\psi_{g1},\ \psi_{g2}, \ldots, \psi_{gD}\} \tag{12}$$

The position and velocity of each particle in the swarm are calculated by Eqs. (13) and (14), which are determined for the iteration that is composed of particle experience and inertial weight.

$$X_i(t) = \{x_{P1},\ x_{P2} \ldots x_{PD}\} \tag{13}$$

$$V_i(t) = \{v_{P1},\ v_{P2} \ldots v_{PD}\} \tag{14}$$

For each iteration number, the particles are evaluated according to a quality assessment, or journey performance, which is called the fitness function, which assigns a fitness value to each particle i, and is calculated by Eq. (15).

$$f(i) = \{w_1|\delta_j{}^Q(i)| + w_2|\delta_{j+1}{}^Q(i)| \ldots w_n|\delta_{j+2}{}^Q(i)|\} \tag{15}$$

where w_n is the weight assigned to each sensitivity, Q is a quality factor taking into account that there is no prioritization between them. On the other hand, the update of the velocity and position of each particle i for each generation by modifying its X_i position, and its velocity V_i towards *Pbest* (ψ_P) and *gbest* (ψ_g). Thus, the updated velocity and position is calculated by means of Eq. (16).

$$V_i^{k+1} = (\varphi v_i{}^k) + a_1\, c_{1,i}(\psi_{P_i}{}^k - X_i^k) + a_2 c_{2,i}(\psi_{g_i}{}^k - X_i^k) \ldots v_{PD} \tag{16}$$

where V_i^{k+1} is the impact that the existing velocity of the particle has on the speed with which it will move to the next position, $\varphi v_i{}^k$ represents inertia, the constants "a" are known as acceleration coefficients, and "c" refers to independent random variables with a uniform distribution. Additionally, Eq. (17) allows the calculation of the next position of the particle, taking into account the velocity.

$$X_i^{k+1} = X_i^k + V_i^{k+1} \tag{17}$$

2.3.2. Repulsive particle swarm (RPS)

The repulsive particle swarm optimization method (RPSO) is a model based on the PSO method that, by increasing its performance when converging in the search space [42], based on the repulsion between the particles, because the PSO model does not guarantee the global optimal when converging, having a large number of optimization parameters and local optimal [43]. This methodology can find the global optimum with Eq. (18).

$$v_i^{k+1} = w v_i^k + c_1 r_1 (p_i^k - x_i^k) + c_2 r_2 w\left(p_j^k - x_i^k\right) + c_3 r_3 w v_r, \tag{18}$$

where, x_i^k and v_i^k represent the position and velocity of particle i at the k^{th} moment, p_i^k denotes a best-local position value found during the k^{th} iteration by particle i, w is an inertial factor. Also, the r_1, r_2 and r_3 are uniform random variables between 0 and 1, while the c_1, c_2 and c_3 are the acceleration coefficients. Finally, v_r indicates the random velocity component, which varies between 0 and 1. Thus, for each particle, the position in the k+1 iteration is estimated from its new velocity using Eq. (19).

$$x_i^{k+1} = x_i^k + v_i^k \tag{19}$$

The implementation algorithm is the same as the one used by the PSO showed in Figure 2. The PSO parameters are presented in Table 2.

Table 2. The RPSO parameters.

Parameters	Value
Maximum iteration	30
Population size	10
Inertial factor, w	0.4–0.9
Cognitive parameters, c_1	1.5
Social parameter, c_2	0.5
Coefficient acceleration	1.5

2.3.3. Genetic algorithm (GA)

Genetic algorithms (GA) are biological algorithms based on evolutionary science, which offer solutions to problems in reality [38], thus obtaining optimal values of the problems, because the algorithm allows a good approach to the problem [39]. Figure 3 shows the representation of the GA algorithm steps, where the main steps are the crossover (Step 6), mutation (Step 7), and selection (Step 5), which are shown as the key phases of the optimization strategy. The growth response is shown in a string (either decimal or binary) called a chromosome, and two maternal strands cross, descendants, or new solutions are created by transferring genes from the chromosomes.

The crossover always has a higher probability, usually 0.8–0.95. The mutation, on the other hand, can be done by flipping a few digits of a string, which generates alternative solutions. The possibility of mutation is low, from 0.001 to 0.005. The new solutions of each generation are evaluated according to the idea of the same solution, which is linked to the objective function of the optimization problem. These new solutions are chosen based on the best solutions in the population and are passed to the next generation with few changes, directly to the process called elitism (Step 8) [40]. Finally, the criterion for the completion of the GA is to define the maximum number of interactions that the process can have. The parameters of the optimization algorithm considered in this study are shown in Table 3.

2.3.4. Performance indicators

Since the analyses of single-objective algorithms start with random populations and all operators are probability-based, it is important to evaluate the performance of these algorithms in many ways since a single measurement cannot determine the correct performance of these with respect to others. Therefore, objectives criteria such as proximity, diversity, and consistency must be met to determine how "ideal" the algorithm can be. The diversity allows knowing the compensations between the objectives that are being compared and those that are in conflict, the coherence shows if the algorithm can find all the regions of the space of ideal solutions.

For the evaluation of the indicators for the fulfillment of the objectives, the Elapsed Time will be used, which is the computational time expended by each swarm intelligence algorithms to find the ideal solution. Another indicator used in this comparative analysis is the root mean square error (RMSE) defined by Eq. (20), where the objective is to minimize the iterative output value (x_t) in the numerical computation, and the optimized last value ($\widehat{x_t}$) at the end of the N population.

$$RMSE = \sqrt{\frac{1}{N}\sum_{t=1}^{N}(x_t - \widehat{x_t})^2} \tag{20}$$

For each of the algorithms, the diversity $S(t)$ is also evaluated according to Eq. (21), which is the Euclidean distance between the possible solutions, allowing the algorithm to be exploited and explored.

$$S(t) = \frac{1}{N}\sum_{t=1}^{N}\sqrt{\sum_{t=1}^{N}(x_t - \widehat{x_t})^2} \tag{21}$$

Parametric and non-parametric tests are performed in order to demonstrate a statistical hypothesis, indicating which optimization strategy is better (parametric) or to show differences between samples (non-parametric). To determine which swarm intelligence algorithm is the best for the energy and exergy optimization problem, a parametric statistical test is done to compare the three algorithms PSO, RPS, and GA for the Brayton S-CO_2-ORC system. The statistical test Z is used for the parameters selected in Table 4.

The null hypothesis (Ha) in this study is a hypothesis that means that there is no statistical significance with a confidence level of 95% between the two optimization algorithm according to the performance indicator selected. Thus, the alternative hypothesis (H_0) is the motivation researcher tried to disprove and is accepted for the cases when there is a difference statistically significant between the two test samples. The study was developed using a Z test calculated from Eq. (22), for the problem to maximize thermal efficiency and minimize destroyed exergy with and without reheat in the Brayton system. The rejection zone, according to the values of Table 4, consists of the values less than 1.64.

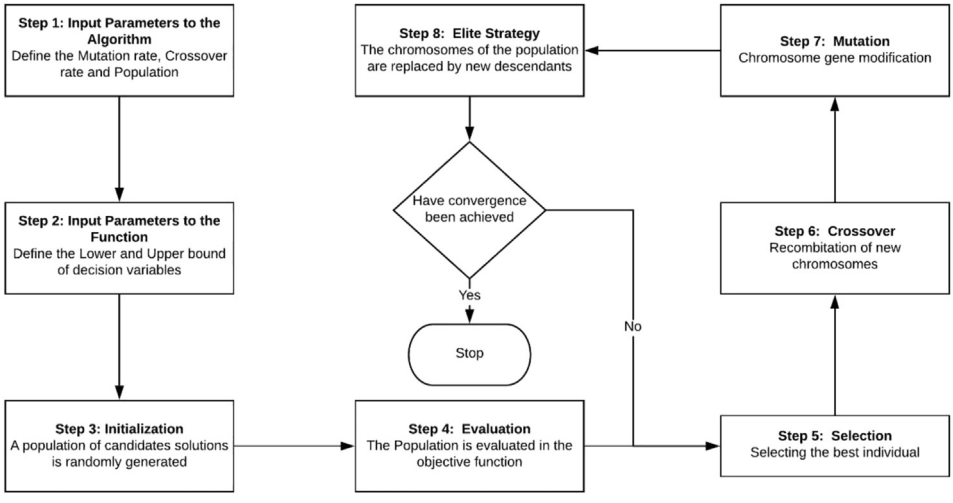

Figure 3. GA flowchart.

Table 3. Parameters of genetic algorithm.

Parameters	Value
Maximum iteration	30
Population size	10
Crossover factor	0.7
Mutate factor	0.3
Mutate rate	0.1
Selection mode	Random

Table 4. Parameters for the statistical parametric z-test.

Parameters	Value
Confidence level	95%
Alpha	0.05%
H_a	$\mu_1 = \mu_2$
H_0	$\mu_1 \neq \mu_2$
Critical Value	1.645

$$Z = \frac{(\overline{X}_1 - \overline{X}_2) - (\mu_1 - \mu_2)}{\sqrt{\frac{\sigma_1^2 - \sigma_2^2}{N}}} \quad (22)$$

3. Results and discussions

3.1. Thermal analysis of the Brayton S-CO_2 - ORC

The thermodynamic analysis of the ORC system as a bottoming cycle of the Brayton supercritical CO_2 cycle was developed, attending to properties presented in Table 5 [5].

Considering the values described above, the thermodynamic properties for each cycle were obtained. In this case, Table 6 shows the values in each current of the organic fluid in the SORC system, Therminol 75 as working fluid in the thermal oil circuit, and CO_2 for each state of the Brayton S-CO_2 cycle.

Based on the values shown in Table 6 for each thermodynamic state of the SORC system in which toluene was used as the working fluid, the exergy balance for each component was developed, and Table 7 shows the different exergy destruction values according to the fuel and product approach.

For the integrated system Brayton S-CO_2 - SORC with and without reheater, the exergy destroyed is greater for the heat exchanger equipment, and these are greater for the Brayton S-CO_2 system operating with reheater, which is due to the effect of operation at higher temperatures that increase the heat transfer irreversibilities. Also, the evaluation of the exergy destroyed in the thermal source in both systems under the engine operation condition, revealed that the system without reheater presents a value of 97 kW, which corresponds to the highest value of exergy destroyed from the devices studied. These results are due to the increase in the entropy production, since in the expansion stage of the system through the two turbines without reheater, greater flow, and energy supply is required to reach the power levels of the turbine for the case with overheating, and therefore a greater exergetic efficiency of the system is obtained.

3.2. Results of the traditional exergetic analysis

The exergy destruction for each component of the SORC and Brayton S-CO_2 integrated system with and without reheater was calculated is presented in Figure 4. The values for the components of the Brayton S-CO_2 cycle are shown in Figure 3a, where there is greater exergy destruction in the thermal source when Reheater is not used, which means a relative difference of 92.28% respect to the results obtained when this component is incorporated.

On the other hand, exergy destruction of approximately 11 kW is observed for the recuperator heat exchanger, achieving a 1.84% increase in exergy destruction when Reheater is not used. In addition, it was observed the zero-exergy destruction value for the secondary turbine because, in this component, the pressure ratio was not significant when not using Reheater. Also, the results for the SORC cycle are presented in Figure 4b, where higher exergy destruction is observed in the heat exchanger, observing a value of 6.5% higher than the system when not using Reheater. Similarly, it is inferred that the second component with the highest exergy destruction is the condenser with a percentage of 15.02% higher when using the Reheater. Thus, these research results show the existence of system parameters for optimal operation, type of organic working fluid, type of ORC and Brayton configuration, the value of temperature pinch in the evaporator and condenser in the ORC, type of heat exchangers, operational parameters of the Brayton as the high pressure and temperature, in addition to the size of the other system components, which are specific to the application studied and motivated the development of the parametric study presented as follow.

3.3. Energy and exergy parametric study

Table 8 presents the values of the decision variables considered to develop energy and exergy optimization. These selected values allowed an appropriate performance in the process.

Table 5. Basic operating conditions for Brayton S-CO_2- SORC systems [5, 6, 7].

System parameters used in Brayton-ORC			
Configuration	Parameter	Value	Unit
SORC	Turbine isentropic efficiency	80	%
SORC	Pumps isentropic efficiency	75	%
SORC	Cooling water temperature	50	°C
SORC	Condenser Pinch Point	15	°C
SORC	Pressure ratio P1	2.5	-
SORC	Evaporators Pinch Point	35	°C
SORC	Pressure ratio P2	30	-
Brayton	Turbine Inlet Temperature	550	°C
Brayton	Brayton Cycle High Pressure	25	MPa
Brayton	Efficiency Brayton Turbines	93	%
Brayton	Compressor Efficiency	89	%
Brayton	Effectiveness of the exchanger	95	%
Brayton	Minimum temperature of Pinch Point	5	°C

Table 6. Thermodynamic properties for S-CO_2-SORC system.

	State	T [K]	P [kPa]	h [kJ/kg]	S [kJ/kg K]	Ė [kW]
SORC	St.16	340.23	4086.31	27.16	0.25	2.31
	St.16 f	498.76	4086.31	462.77	1.28	31.41
	St.16 g	498.76	4086.31	613.94	1.58	45.50
	St.12	530.95	4086.31	745.82	1.84	58.29
	St.13	392.70	136.21	599.53	1.94	16.62
	St.14	392.70	136.21	599.53	1.94	16.62
	St.15	338.15	136.21	511.47	1.69	13.09
Thermal Oil	St.9	565.95	101.43	427.43	0.90	66.34
	St.9 g	477.94	100.02	236.97	0.58	19.45
	St.9 f	447.40	98.55	175.21	0.45	8.91
	St.10	420.75	68.15	123.42	0.34	2.58
	St.11	420.87	170.38	123.65	0.34	2.60
	St.17	317.15	101.30	184.33	0.19	3.33
	St.18	328.15	101.30	230.33	0.33	10.37
	St.19	330.12	101.30	238.57	0.36	12.03
Brayton S-CO_2	St.1	923.15	25000.00	1157939.25	2837.79	621989.00
	St.2	851.47	14838.74	1073770.62	2845.26	535595.29
	St.3	923.15	14838.74	1162647.92	2945.47	594594.68
	St.4	822.63	6956.21	1044993.60	2956.28	473716.27
	St.5	468.21	6956.21	637942.14	2311.47	261179.92
	St.6	328.65	6956.21	464580.68	1867.04	218061.45
	St.7	445.25	25000.00	540232.48	1885.84	288108.24
	St.8	758.87	25000.00	951395.57	2591.49	488881.97

Table 7. Exergy analysis results for each component.

System	Components	φ_F[kW]	φ_P[kW]	φ_D[kW]	φ_L[kW]	φ_F[kW]	φ_P [kW]	φ_D[kW]	φ_L[kW]
		Reheater				No Reheater			
SORC	Heat Exchanger	53.72	33.26	20.46 1	-	47.75	19.13	19.13	-
	Pump 1	0.15	0.02	0.12	-	0.16	0.13	0.13	-
	Turbine	30.39	25.87	4.51	-	28.42	4.32	4.32	-
	Pump 2	0.24	0.19	0.05	-	0.23	0.05	0.05	-
	Evaporator	53.75	47.67	6.07	-	47.78	4.17	4.17	-
	Condenser	17.47	8.46	9.01	-	15.37	7.65	7.65	-
Brayton S-CO_2	Compressor	60.69	55.99	4.69	-	50.41	4.03	4.03	-
	Turbine primary	68.85	66.88	1.97	-	142.77	4.48	4.48	-
	Turbine secondary	94.65	91.85	2.79	-	0.00	0.00	0.00	-
	Recuperator	163.74	152.54	11.20	-	141.28	11.41	11.41	-
	Thermal source	53.28	45.79	7.48	-	235.00	97.00	97.00	-

The effect of the turbine inlet temperature ($\mathbf{T_{IT}}$), recuperator efficiency ($\varepsilon_{\mathbf{ff}}$), primary turbine efficiency ($\boldsymbol{\eta}_{\mathbf{T1}}$), evaporator pinch point (**AP**), evaporator pressure (P_{evap}), and high pressure (P_{HIGH}) on the overall thermal efficiency and exergy destruction are studied for the different configurations of the S-CO_2-SORC system with and without superheater, as shown in Figure 5.

The effect of the inlet turbine temperature (T_{IT}) on the global thermal efficiency and exergy destruction is presented in Figure 4a, where approximately a constant value of 53% of global efficiency is evidenced for the system without reheater, and a considerable increase in the global efficiency is presented for the system with reheater, achieving about 58% at a T_{IT} of 850 °C. On the other hand, the exergy destroyed is conserved in small values (93 kW) for the system with reheater. However, when using a reheater, the exergy destroyed increases as the T_{IT} increases, obtaining a value close to 225 kW. Therefore, it can be deduced from the results that for the system that does not use a reheater, the efficiency is maintained at an attractive value, and the exergy destruction is kept at minimum values, which could facilitate the worldwide implementation of these systems in a real industrial operational context.

In addition, as the recuperator efficiency ($\varepsilon_{\mathbf{ff}}$) increases, proportionally increase the overall thermal efficiency and the total exergy destruction decreases as shown in Figure 4b, where the overall efficiency without reheater (NRH) is 2.2% lower than the value obtained for the system with reheater (RH), and the exergy destruction is higher 13.53% with the use of reheater (RH) at 80% in the recuperator efficiency. These results show that from an energy point of view, the addition of a reheater is technical beneficial; however, the addition of a heat exchanger involves the enhancement of the heat transfer irreversibilities that cause greater exergy destruction. Thus, it is suggested to develop thermoeconomic studies that allow obtaining an optimal configuration and operation conditions for this integrated thermal generation system.

Also, an increase in the turbine 1 efficiency, which is the primary turbine of the Brayton cycle, implies and enhancement in the cycle overall efficiency with reheater, as shown in Figure 5c. Besides, this value

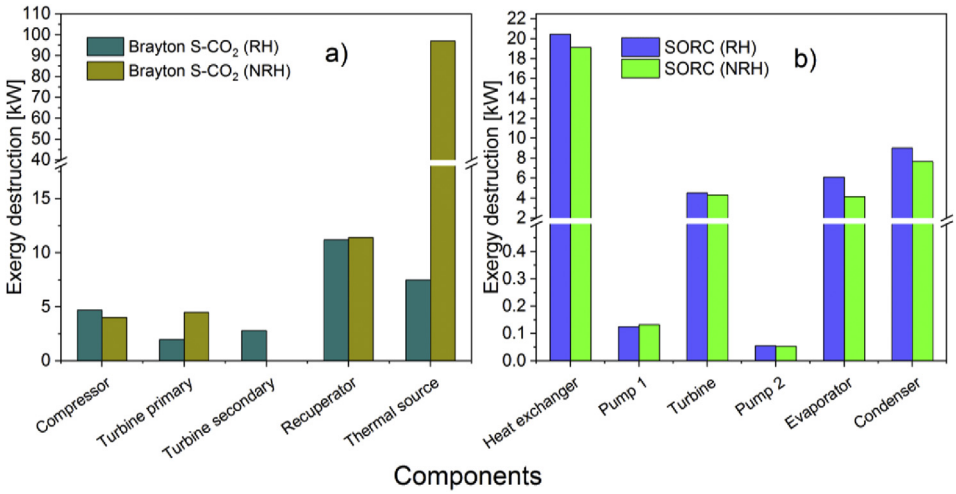

Figure 4. Exergy destruction fraction for each component.

Table 8. Range of decision variables.

Variables		Brayton S-CO_2-SORC	
Symbol	Units	Minimum	Maximum
T_{IT}	°C	500	800
ε_{ff}	%	70	95
η_{T1}	%	70	95
AP	°C	15	35
P_{evap}	MPa	0.45	3.55
P_{HIGH}	MPa	20	30

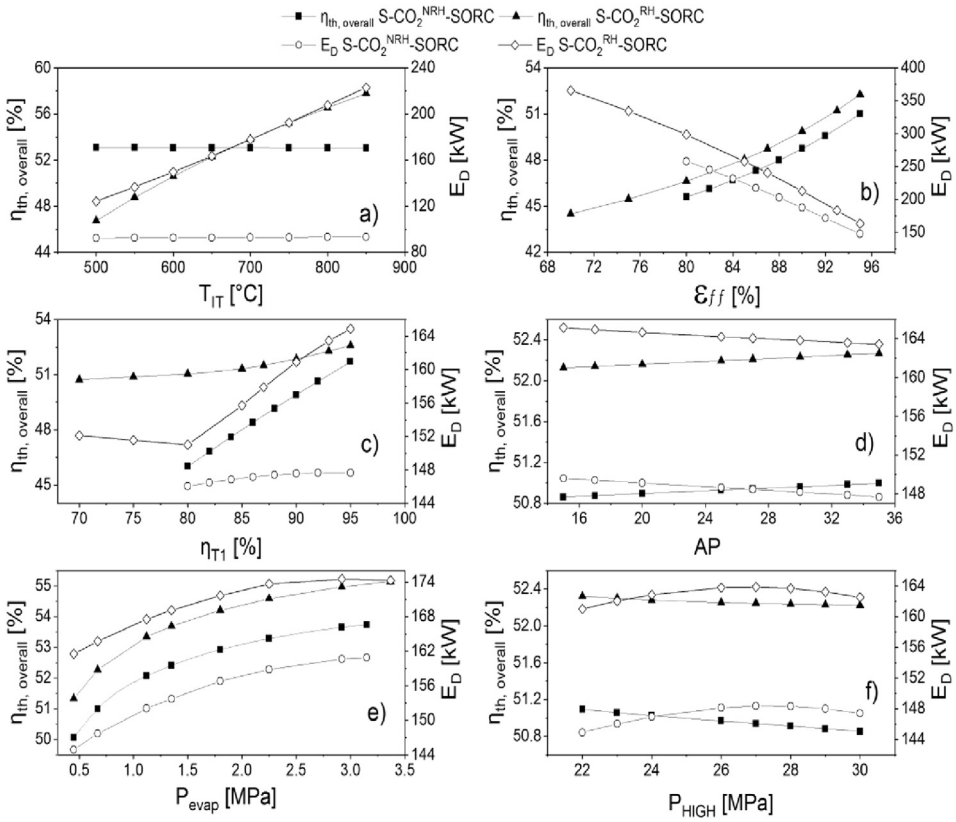

Figure 5. Overall thermal efficiency and total exergy destruction as a function of the (a) turbine inlet temperature, (b) recuperator efficiency, (c) primary turbine efficiency, (d) evaporator pinch point, (e) evaporator pressure, and (f) high pressure.

is higher than the results obtained without reheater (NHR), and the exergy destruction for the system with reheater presents a decrease when the turbine 1 efficiency increase from 70% to 80%. Therefore, the turbine efficiency is a relevant variable to consider in the energy and exergy optimization approach and should also be considered in thermo-economic studies because of the purchase equipment cost, and thermo-economic indicators of these systems are a function of the power generated and efficiency.

From the parametric results presented in Figure 5d, where the effect of the evaporator pinch point (AP) on the overall thermal efficiency and total exergy destruction is studied, is observed greater efficiency and equally more significant exergy destruction with the Brayton cycle operating with reheater (RH). However, it is clear that as AP increases, exergy destruction decreases for the integrated system with and without reheater, which directly affects the amount of evaporated organic fluid available for expansion in the ORC turbine, and the heat transfer area required for the evaporator. The evaporator pinch point is defined as the minimum temperature difference between the thermal oil and the organic working fluid in the evaporator. This value increase at constant operation parameters of the process leads to an increase in the energy generated by the integrated system using toluene as the organic working fluid, which is explained by the thermal proximity between the organic fluid and the thermal oil.

Figure 5e shows an increase in evaporator pressure (Pevap) that leads to higher system efficiency when using a reheater, and lower exergy destruction when not using a reheater, establishing that for a Pevap of 2.25 the overall thermal efficiency is 2.4% lower without the use of a reheater, and the exergy destruction is 8.6% higher with the use of a reheater. Thus, these results are due to the fact that the configurations that use the reheater have lower total exergy losses, with a decrease of around 10% in the high temperature of the system. In addition, both the configuration with and without reheating, the highest exergy losses are presented by the exergy gained by the cooling CO_2 and heat transfer in the heat source, as these are included for the case of configuration with reheating between 14% and 18% of total losses, while for configurations without reheating, exergy losses due to exergy gained by air and heat source are in the range of 12% and 15% of total losses.

Finally, when increasing the high pressure (PHIGH), a small decrease in overall thermal efficiency was achieved with and without reheating, as shown in Figure 5f. Also, in the case of exergy destruction, a reduction is shown when the high pressure is greater than 26 MPa for both cases of with and without reheating. This is because operation in the compression and expansion stages occurs at lower pressure ratios, and therefore power generation is reduced. Thus, this operational parameter plays an important role in the energy and exergetic optimizations of this type of integrated system.

3.4. Optimization of the integrated S-CO_2 – SORC system with and without reheater

An analysis of the thermal efficiency (η_{th}) and exergy destroyed (E_D) behavior for the integrated S-CO_2-SORC system was carried out with and without reheater, taking into account four different numbers of particles, and 30 iterations, in which the value of the particles and iterations number that maximizes the thermal efficiency and minimizes the total exergy destruction are studied. Figure 6 presents the results obtained in the optimization study with the PSO algorithm.

According to the results presented in Figure 6a, in which a maximization of the thermal efficiency for the Brayton S-CO_2- SORC system without reheater (NRH) was obtained, the maximum thermal efficiency of 55.53% is achieved when 19 is the number of iterations, and 25 is set as the number of particles. Likewise, in Figure 6b, the same analysis is shown for this case, but with reheater (RH), and it is observed that for a 25 in the number of particles and an iteration value of 11, a maximum value of efficiency of 56.95% is obtained. These results are quite promising due to the levels of thermal efficiency achieved allows thinking about a wide application of these systems for energy self-generation in industrial environments, once their technical and economic feasibility is evaluated and guaranteed.

On the other hand, it is sought to optimize the system by mean of the total exergy destruction minimization, as shown in Figure 6c, where it is observed that the lower value obtained in the total exergy destruction was 60.72 kW (NRH) with 6 iterations and 15 in the number of particles. Likewise, for the case presented in Figure 6d, the minimization of total exergy destruction was obtained at the iteration 6, and 20 in the particle number, which achieved the lowest the total exergy destruction value in the system (RH) of 112.06 kW.

The decision variable behavior when the maximum thermal efficiency of 55.53% is obtained for the supercritical CO_2 cycle without reheater, and particle number of 25 (Solution I), is presented in Figure 7. The decision variables presented are the turbine inlet temperature (T_{IT}), and the high pressure (P_{HIGH}) in Figure 7a, the recuperator effectiveness (ε_{ff}), and the primary turbine efficiency (η_{T1}) in Figure 7b, the evaporator pinch point (AP), and the evaporator pressure (P_{evap}) in Figure 7c. The same decision variables were studied for the system with reheater and particle number of 25 from Figure 7d–f (Solution II), where the higher thermal efficiency of 56.95% was achieved.

Figure 7a shows that the temperature at the turbine inlet increases steps by step until iteration 8, then the value remains stable at approximately 800 °C, in parallel with the high pressure (P_{HIGH}) begins to drop considerably to 20000 kPa. Therefore, the tendency for better system performance is obtained at higher high inlet turbine temperatures, and high pressures at medium values in order to have pressure ratios that do not increase the heat transfer irreversibilities in the compression and expansion equipment.

In Figure 7b, the effectiveness of the recuperator increases up to an iteration number of 4 achieving 90%, and in the same way, the turbine efficiency increased until it stabilized in 92.8% with a number of iterations of 7. This result is due to the nature of the objective functions considered in the optimization since these by not considering economic aspects such as the purchase equipment cost assigns the efficiencies of these devices to the upper limit considered in the PSO optimization.

From the results presented for the AP and P_{evap} as shown in Figure 7c, it is observed that the two variables show a decrease in the first iterations and then increase step by step, giving rise to a stabilization in the evaporator pinch point in 35 °C, and in the evaporator pressure is 2.9 MPa. The initial behavior of these variables is due to the need to have an evaporator pinch point as low as possible at low turbine inlet temperatures, to achieve the best possible thermal performance of the integrated system.

Then, the analysis for the system with superheat (RH) is shown in Figure 7d, where the temperature at the turbine inlet considerably increases until iteration 10 at a temperature of 800 °C, then the value remains stable, while the high pressure (P_{HIGH}) begins to increase in the first iterations up to 25000 kPa, then decreases until iteration 13 where a pressure of 20000 kPa is stabilized, which is a similar result to the obtained with the NHR system. Therefore, the most important variable in the thermal performance of an integrated supercritical CO_2 Brayton – ORC system is the temperature and pressure reached by the CO_2 at the inlet turbine. Thus, additional research should be done on more efficient printed circuit heat exchange systems that do not generate so many heat transfer irreversibilities. Besides, in Figure 6e, f it is evidenced by the same behavior presented by the NHR.

The decision variable behavior in the analysis of the integrated supercritical CO_2 cycle without reheater and ORC for the number of particles in 15 that achieved the lowest exergy destruction with 60.72 kW (result presented in Figure 6c) is related to the solution III and presented from Figure 8a–c, while the Solution IV presented from Figure 8d–f is related to the integrated system with reheater for the number particles of 20 to achieve the lower exergy destruction with 112.06 kW (result presented in Figure 6d).

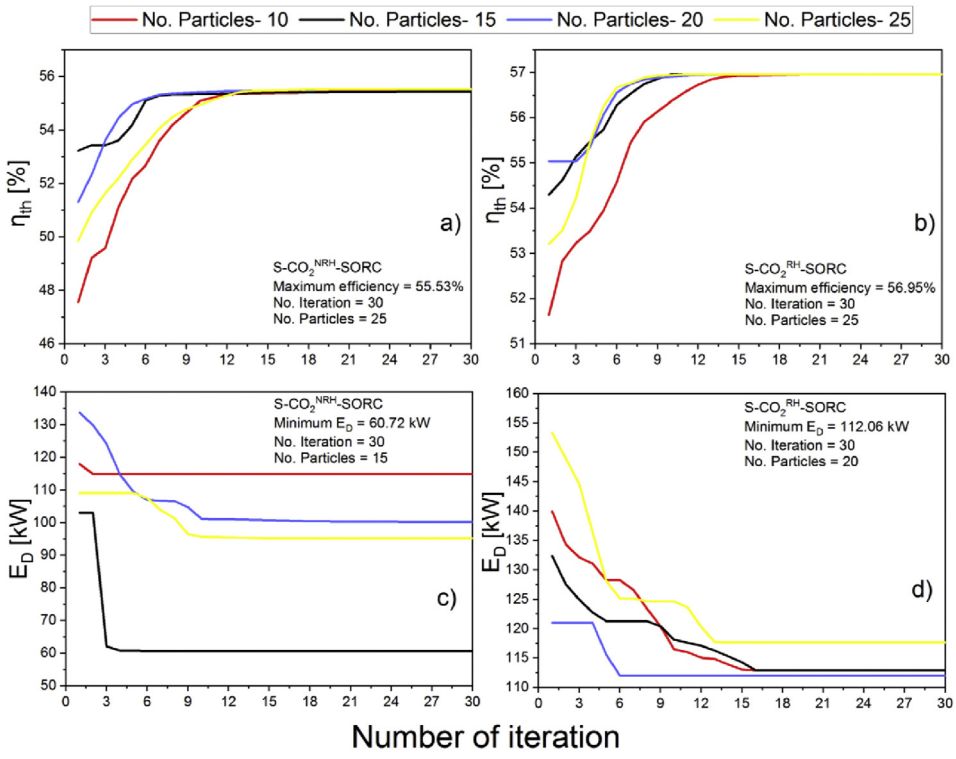

Figure 6. Respond of the thermal efficiency and exergy destroyed with the number of iterations and particles of a Brayton S-CO_2- SORC combined system with and without reheat for (a) Maximum efficiency without reheat, (b) Maximum efficiency with reheat, (c) Minimum exergy destruction without reheat, and (d) Minimum exergy destruction with reheat.

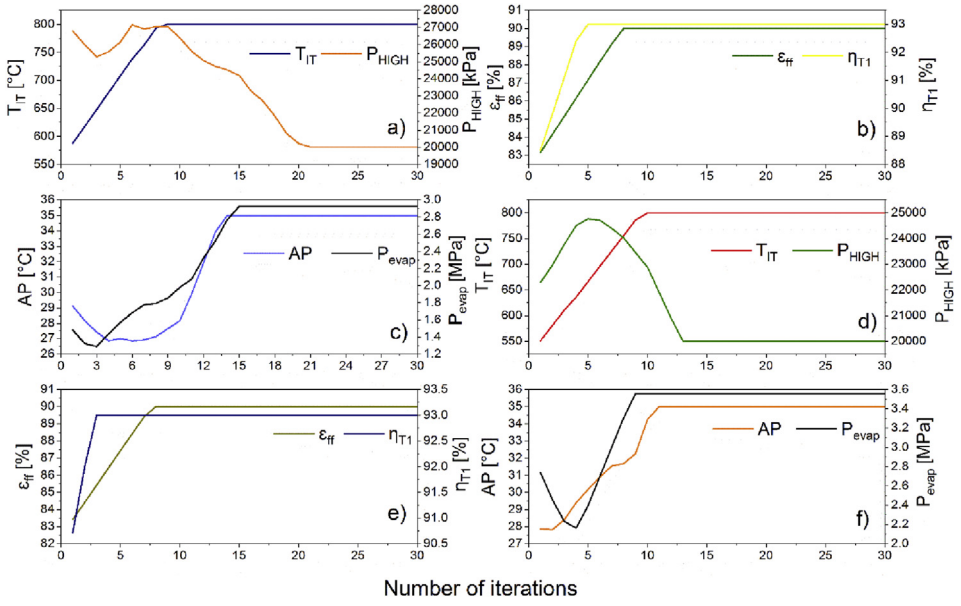

Figure 7. Decision variables for a particle number of 25 in the system without reheater (NRH) (a) T_{IT} and P_{HIGH}, (b) ε_{ff} and η_{T1}, (c) AP and P_{evap}, system with reheater (RH) (d) T_{IT} and P_{HIGH}, (e) ε_{ff} and η_{T1}, (f) AP and P_{evap} as a function of the number of iterations.

For solution III as shown in Figure 8a, it is observed that stabilization was achieved at a lower iteration number compared to the solution I (Figure 7a) where the turbine inlet temperature (T_{IT}) decreases considerably at 500 °C, and the high pressure (P_{HIGH}) increases to 30000 kPa at an iteration of 5. Therefore, when the optimization method considers the total exergy destruction as an objective function, the PSO method spends fewer iterations to reach convergence and optimal values.

For the case of Figure 8b, it is observed that the efficiency of the recuperator suddenly increases to 90% at an iteration of 2. Similarly, the efficiency of the turbine at an iteration of 8 stabilized at a value of 90%. On the other hand, an oscillatory behavior was reflected in the AP variable presented in Figure 8c, in which it was not possible to reach a stable value. However, in the iteration of 27 a small AP oscillation is observed between 16.0 °C and 16.2 °C, and in the case of the evaporator

pressure, it remains stable at the iteration value of 4 to a value of 0.46 MPa.

In Table 9, four solutions are presented according to the simulations results presented related to the operating conditions of the Brayton S-CO_2-SORC integrated system. A comparative study was carried out between the solutions to obtain maximum thermal efficiency for the Brayton system with (Solution II) and without Reheater (Solution I). Also, the comparative study for the minimization exergy destruction problem was considered with (Solution IV) and without Reheater (Solution III) in the Brayton system. The maximum power (234.72 kW) was obtained when the thermal efficiency with Reheater is maximum, which approximately doubles the power obtained while the exergy destruction in the system is minimized. Therefore, considering that the technical and economic viability of these systems is reached with the greater production of energy, it is suggested to orient the technological efforts in increasing the thermal performance of the integrated thermal system in the first instance and then to identify the components that have more opportunities of exergetic improvement due to the high heat transfer irreversibilities that occur in this equipment.

The main contribution of this research is to find opportunities for improvement through genetic algorithm optimizations using exergetic analysis as an input variable by changing the operating conditions of the thermal cycle. However, it is recommended to implement thermo-economic analyses to expand the range of the study and find more variables of opportunity, using indicators such as the LCOE and focusing on variables based on exergy analysis [41]. The inclusion of these thermo-economic indicators in the objective variables will allow obtaining a Brayton S-CO_2-SORC thermal generation system optimized thermo-economically in real operation contexts, where the ORC behaves as a glue cycle that favors the technical and economic viability for its commercial application. This viability is due to the use of residual heat from the Brayton S-CO_2 cycle, since the availability of energy contained in the CO_2, and the amount of additional energy that could be generated with the use of ORC without additional fuel consumption, provide the opportunity to reduce energy costs of generation, achieve shorter payback periods and reduce environmental impacts associated with the system [41].

Furthermore, it is recommended to use environment variables, which can be taken from methodologies based on Eco-99 method such as the life cycle analysis (LCA), methodologies with exergetic analysis such as traditional and advanced exergetic-environmental analysis. Theses methodologies allow to evaluate and describe the thermodynamic properties, the energy duty of the equipment, and the improvements potential of the components from a thermodynamics second law point of view, including the potential environmental impact in all the LCA phase, which are the construction, operation and decommissioning of the system.

3.5. Comparative performance of different swarm intelligence algorithms

A complementary analysis of the thermal efficiency and exergy destruction behavior is performed for the integrated S-CO_2-SORC system considering the reheater and without it. For this, the RPS and GA algorithms were taken into account from the swarm intelligence algorithms, with the parametric conditions proposed in Tables 2 and 3, respectively. Also, the results presented in Figure 5 for the PSO algorithm was considered for the number of iterations 30. This analysis is based on the results of Figure 6 and takes the same operating conditions: maximizing thermal efficiency and minimizing exergy destruction in the three algorithms presented and observing their convergence with respect to the iterations proposed. The results obtained from this analysis are presented in Figure 9.

According to the results shown in Figure 9, the maximum thermal efficiency that can be achieved in a system with a reheater (Figure 9a) and without a reheater (Figure 9b) was evaluated, as well as the minimum value in the exergy destruction with (Figure 9c) and without (Figure 9d) reheater. In Figure 9a a maximum thermal efficiency of the system with reheater of 56.95% was obtained in iteration number 19 for the PSO algorithm, which was shown to have the faster convergence and stability, respect to the RPS and GA algorithms, which reached a thermal efficiency value of 55.95% and 54.45%, respectively. These results are due to the rapid convergence of the PSO algorithm, compared with the other global optimization algorithms, such as GA and RPS, in addition to its easy implementation, simplicity in its optimization strategy, and it is the most efficient global search algorithm among those studied with the best computational efficiency.

The maximum thermal efficiency of 55.53% for the PSO algorithm was obtained for the thermal system with reheat, as shown in Figure 9b, 54.53% for the RPS algorithm, and 53.09% for the GA algorithm. This shows the good performance of the PSO algorithm in thermal system

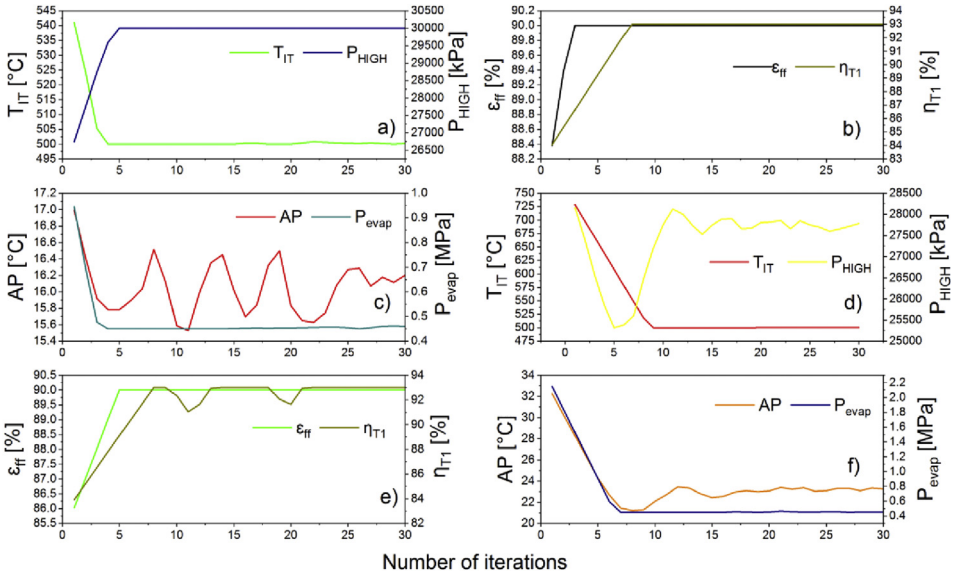

Figure 8. Distribution of decision variables for a particle number of 15 (NRH) (a) T_{IT} and P_{HIGH} (b) ε_{ff} and η_{T1} (c) AP and P_{evap} and a particle number of 20 (RH) (d) T_{IT} and P_{HIGH} (e) ε_{ff} and η_{T1} (f) AP and P_{evap} as a function of the number of iterations.

Table 9. Thermal optimization solution in the Brayton S-CO_2-SORC.

Parameter		Optimized Value			
Symbol	Unit	Solution I (NRH)	Solution II (RH)	Solution III (NRH)	Solution IV (RH)
		Maximize thermal efficiency		Minimize exergy destruction	
T_{IT}	°C	800.00	800.00	500.21	500.23
P_{HIGH}	kPa	20000.00	20000.31	30000	27781.70
ε_{ff}	%	0.9	0.9	0.9	0.9
η_{T1}	%	0.93	0.93	0.93	0.93
AP	°C	35	35	16.20	23.27
P_{evap}	MPa	2.92	3.55	0.45	0.45
$\Delta\eta_{ther}$	%	28.26	27.34	26.40	26.85
$\eta_{I,SORC}$	%	21.03	21.44	15.08	14.94
$\eta_{I,\ Brayton\ S-CO2}$	%	43.29	44.72	33.71	34.56
$\eta_{th,overall}$	%	55.53	56.95	42.61	43.84
E_D	kW	62.04	121.47	60.72	112.06
$\dot{w}_{net}$	kW	200.87	234.72	109.34	116.46

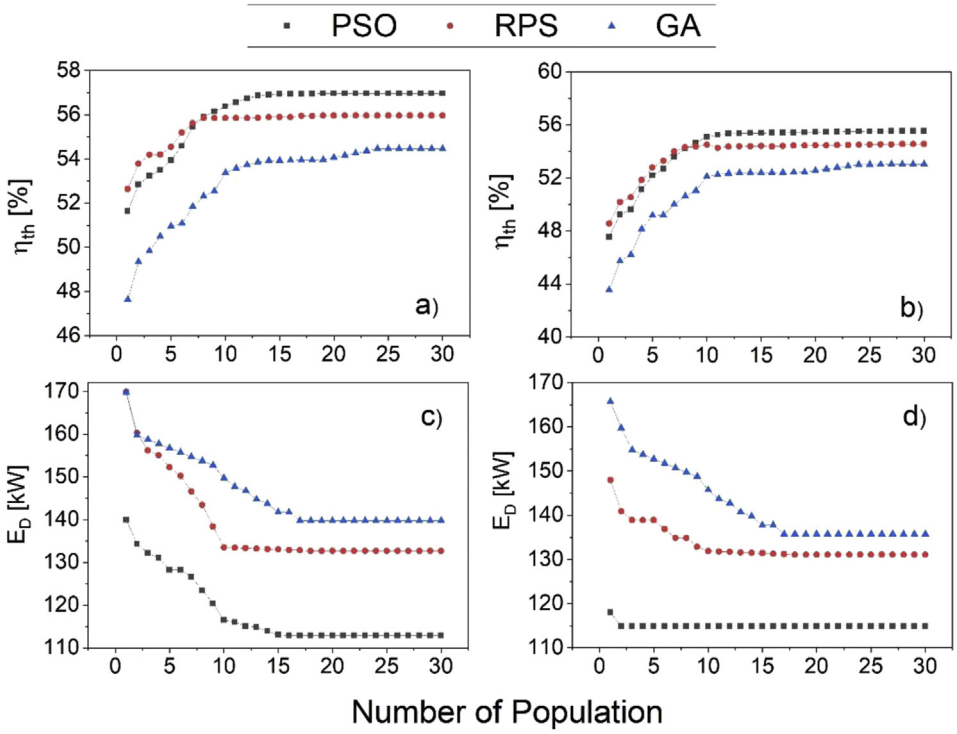

Figure 9. Optimization result with the three swarm intelligence algorithms for (a) Maximum efficiency without reheat, (b) Maximum efficiency with reheat, (c) Minimum exergy destruction without reheat, and (d) Minimum exergy destruction with reheat.

optimization, which is promising for implementation in self-generated energy applications, and that it is the right algorithm to use in those environments due to its local convergence. Additionally, the deviation of the RPS algorithm can be explained by the facility of this algorithm to fall into optimal local values within the high dimensional search space, and the comparatively low convergence ratio in the iterative optimization process developed in the energy efficiency maximization, regardless of whether the system has reheater.

On the other hand, in Figure 9c are shown the minimum value of exergy destruction for the PSO algorithm (112.95 kW) without reheat, RPS algorithm (132.72 kW), and GA algorithm (139.73 kW), while in Figure 9d, it is shown that the minimum exergy destruction obtained with the PSO algorithm (114.88 kW), RPS algorithm (131.37 kW), and GA algorithm (135.73 kW). In these processes of exergy destruction minimization, better results can be obtained for the GA algorithm by extending the population size, but in this study, due to its computational implementation, a finite equal size (30) has been limited for the three methods. In addition, it is demonstrated that with the use of an incorrect objective function in these problems, it is possible that the algorithm is not able to find a correct solution to the problem or the best-operating conditions of the system in terms of energy or exergy approach.

In this case, the same result is presented for Figure 9a, b, where the PSO algorithm is shown to have the best performance reaching the optimal value in iteration number 3. For this reason, it is recommended to opt for the PSO, which has had greater acceptance due to its easy algorithmic implementation among the optimization strategies studied, despite the fact that both (PSO and GA) were proposed by almost a year.

Once the comparisons between the algorithms were made, the performance indicators were evaluated, with the aim of showing which is the ideal algorithm for the integrated S-CO_2-SORC system. Three

indicators were evaluated, as shown in Figure 10, for the cases of maximizing the energy efficiency and minimizing the exergy destruction with and without reheater: Elapsed Time (Figure 10a and 10b), RMSE (Figures 10c, d) and Diversity (Figure 10e,f).

For Figure 10a, it is shown that for the algorithms evaluated with reheater, the elapsed time takes values of more than thousands above the values of elapsed time without reheater, this shows that the inclusion of reheater in the algorithm considerably affects the response time for obtaining computational results, which is a consequence of the computational algorithm loop and thermal system complexity. Similarly, Figure 10b shows that the response time of the PSO algorithm is reduced for both the integrated system and the integrated system without reheater in comparison with the other algorithms evaluated, which is favorable for the evaluation of exergy destruction reduction.

Also, the results of root mean square error performance indicator is shown in Figure 10c for the three algorithms evaluated, where it is observed that the GA algorithm is the one that reduces the least its value with respect to the other algorithms studied, so this algorithm should not be used for energy and exergetic optimization problems of S-CO_2-ORC thermal systems since in addition to consuming significant computational time in its execution and computational power, reaches values with higher mean square errors than alternatives such as PSO and RPS.

Figure 10d shows that the highest RMSE reduction is observed in the PSO algorithm for the integrated system without reheater, which is shown as the favorable optimization algorithm option due to the fulfillment of the objective for this thermal case study. In addition, Figure 10e shows the PSO algorithm for evaluation with reheater with the least diversity value among the remaining algorithms, showing it as a strong candidate for the ideal algorithm for the solution of the case. This result is due to the PSO is a blind search method, which is only guided by the selected fitness function, and the particle swarm operators are independent of the selected problem, thus making them general and indifferent to whether the Brayton system has a reheater or not integrated to the ORC.

Figure 10f shows the diversity for the case of minimum exergy reduction between the three algorithms with reheater and without reheater, where the algorithms behave similarly, with the highest diversity for the algorithms implemented to problems without reheater. However, these results are due to the algorithm computational structure since in this study, parameters were selected that guarantee the diversity of the population to have a high representation in the search space and avoid premature convergence in the search for a better energetic and exegetic performance of the integrated system.

To complete the analysis, Figure 11 shows the maximum, minimum, and average values of each performance indicator for the PSO, RPS, and GA algorithms evaluated in the Brayton S-CO_2- SORC combined system with reheater and without reheater.

In Figure 11a, it is shown that the minimum elapsed times between the algorithms were obtained by the PSO without reheater (50.12 s) and RPS without reheater (85.12 s) algorithms. Also, in Figure 11b it is shown as the GA algorithm presented the highest elapsed time values as a consequence of the high complexity of the problem, presenting minimum considering the reheater of 103.13 s, maximum of 1551.64 s, and average 3049.9 s. Figure 11d shows the RMSE values for the studied algorithms, presenting the lowest values for the PSO NRH algorithm, where minimum (0.56), and maximum (0.99) values were obtained. Figure 11f presents values for diversity, where the lowest values were presented for PSO NRH, with a minimum value of 0.10. Therefore, a possible solution for the high complexity problem involved in the optimization of these integrated energy systems may be the use of distributed computer systems, where it is possible to run intelligent swarm algorithms in parallel, where each processing unit can operate in an isolated population of particles, and the best individuals from each isolated population are run in other computer units. This alternative will allow the development of studies of greater complexity, such as the thermo-economic optimizations of these thermal systems that require more computational resources.

3.6. Statistical test

From Tables 10, 11, and 12, the Z values for the statistical test performed is presented for the three optimization algorithms, determining the significance of the proposed mean comparison test, where "S" means that evidence of a significance is found and the null hypothesis must be rejected, while "NS" means that some evidence of significance has not been found and the null hypothesis must be accepted. These tables take

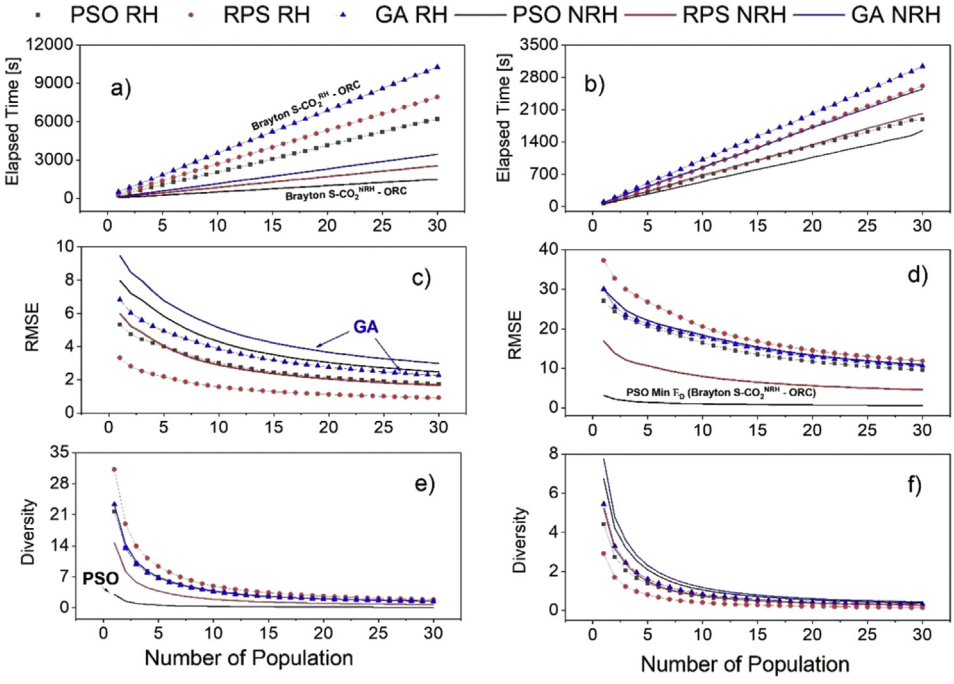

Figure 10. Performance indicator responds for Elapsed time (a) maximum efficiency, (b) minimum exergy destruction, for RMSE (c) maximum efficiency, (d) minimum exergy destruction, for Diversity (e) maximum efficiency, and (f) minimum exergy destruction.

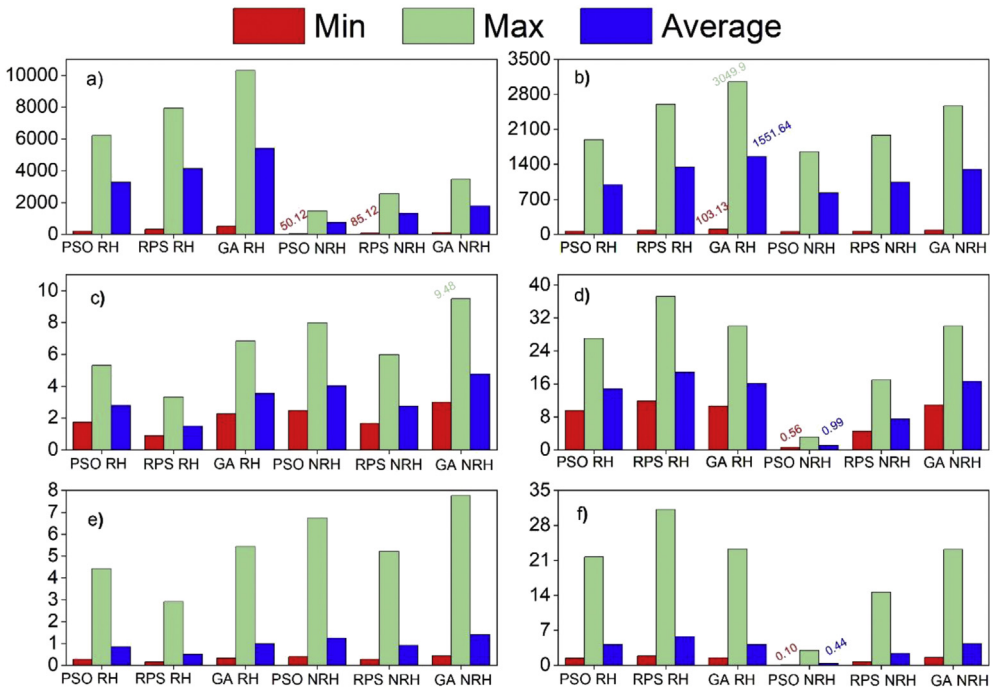

Figure 11. Maximum, minimum and average values of each performance indicator for the PSO, RPS, and GA for (a) Elapsed time for the maximum efficiency, (b) Elapsed time for the minimum exergy destruction, (c) RMSE for maximum efficiency, (d) RMSE for the minimum exergy destruction, (e) Diversity for the maximum efficiency, and (f) Diversity for the minimum exergy destruction.

the algorithm and performance indicator depending on the optimization objective, and each method studied in this thermal configuration.

The hypotheses proposed in this statistical test are presented as follow:

H_o: The mean obtained in the performance indicator (Elapsed time/Diversity/RMSE) using the (PSO/RPS/GA) algorithm for the (maximizing the thermal efficiency/minimizing the exergy destruction) problem in the Brayton S-CO_2-ORC integrated system without reheater and with reheater is statistically equal. H_a: The mean obtained in the performance indicator (Elapsed time/Diversity/RMSE) using the (PSO/RPS/GA) algorithm for the (maximizing the thermal efficiency/minimizing the exergy destruction) problem in the Brayton S-CO_2-ORC integrated system without reheater and with reheater is statistically different.

The statistical test results show that in most cases, there is a significative difference with a confidence level of 95%, with the PSO optimization result different in five tests, which imply to reject the null hypothesis. The least relevance was the GA algorithm, presenting similar results for the performance indicator, including the reheater in the system, mainly for the Diversity and RMSE tests.

4. Conclusions

It was verified that the PSO metaheuristic algorithm has the potential to be used in the optimization of several objective non-linear functions subject to equality or inequality constraints, among which are included the problems of energy and exergetic optimization of the integrated S-CO_2-SORC power generation systems. The PSO, for the cases studied, gave an approximate answer that satisfies the optimization needs and contributes to solving nonlinearity problems present in most engineering and scientific applications. If a very high precision response is required, regardless of the required computational costs, a deterministic method is an appropriate choice for the target functions studied in this paper.

The results obtained in the present investigation allowed to observe that during the maximization of the thermal efficiency in the S-CO_2-SORC system, a value of 56.95% was reached with the use of reheater for a number of particles of 25. Likewise, when deactivating the use of the reheater in the system, the efficiency decreases, reaching a maximum thermal efficiency of 55.53% at the same number of particles with the PSO algorithm, so a 1.42% improvement is obtained when using reheater in a Brayton supercritical CO_2 cycle.

In the case of minimizing exergy destruction, the integrated S-CO_2-SORC system without reheater to a particle number of 15 showed a considerable decrease to a value of 60.72 kW; otherwise, it is presented in the system when using the reheater where an increase of 112.06 kW is seen. Thus, it is suggested to use the system without reheating when a good exergetic performance of the integrated system with an ORC is preferred.

The optimizations developed for the integrated S-CO_2-SORC system allowed to obtain favorable energy indicators of the system when using

Table 10. Results for the statistical test for the PSO optimization algorithm.

Performance Indicator	μ1	μ2	Zvalue	Evidence
Elapsed Time	Min E_D S-CO_2^{NRH}	Min E_D S-CO_2^{RH}	27.10	S
	Max η S-CO_2^{NRH}	Max η S-CO_2^{RH}	286.79	S
Diversity	Min E_D S-CO_2^{NRH}	Min E_D S-CO_2^{RH}	9,40	S
	Max η S-CO_2^{NRH}	Max η S-CO_2^{RH}	-1.50	NS
RMSE	Min E_D S-CO_2^{NRH}	Min E_D S-CO_2^{RH}	32.74	S
	Max η S-CO_2^{NRH}	Max η S-CO_2^{RH}	5.25	S

Table 11. Results for the statistical test for the RPS optimization algorithm.

Performance Indicator	μ1	μ2	Zvalue	Evidence
Elapsed Time	Min E_D S-CO_2^{NRH}	Min E_D S-CO_2^{RH}	45.43	S
	Max η S-CO_2^{NRH}	Max η S-CO_2^{RH}	278.58	S
Diversity	Min E_D S-CO_2^{NRH}	Min E_D S-CO_2^{RH}	6.08	S
	Max η S-CO_2^{NRH}	Max η S-CO_2^{RH}	-1.79	NS
RMSE	Min E_D S-CO_2^{NRH}	Min E_D S-CO_2^{RH}	20.00	S
	Max η S-CO_2^{NRH}	Max η S-CO_2^{RH}	-5.21	NS

Table 12. Results for the statistical test for the GA optimization algorithm.

Performance Indicator	μ1	μ2	Zvalue	Evidence
Elapsed Time	Min E_D S-CO_2^{NRH}	Min E_D S-CO_2^{RH}	34.65	S
	Max η S-CO_2^{NRH}	Max η S-CO_2^{RH}	313.73	S
Diversity	Min E_D S-CO_2^{NRH}	Min E_D S-CO_2^{RH}	-0.26	NS
	Max η S-CO_2^{NRH}	Max η S-CO_2^{RH}	-1.38	NS
RMSE	Min E_D S-CO_2^{NRH}	Min E_D S-CO_2^{RH}	-0.83	NS
	Max η S-CO_2^{NRH}	Max η S-CO_2^{RH}	-3.90	NS

reheater and to select thermal efficiency as the objective function in the optimization approach. The study allowed to obtain promising energy indicators such as the thermal efficiency of the Brayton (44.72%), the thermal efficiency of the SORC cycle (21.44%), and the overall efficiency of integrated system Brayton S-CO_2 - SORC (56.95%), which is a consequence of the reheater and the waste heat recovery in the heat exchanger of the organic Rankine cycle. However, in exergetic terms, this configuration is not the best option because it has heat transfer irreversibilities; so, the total exergy destroyed of 121.47 kW was the highest presented.

It is recommended as future work to include thermo-economic and environmental variables to increase the opportunities for improvement of the input variables and components of the system from the irreversibilities of the components and environmental impacts.

A comparative analysis of the swarm intelligence algorithms response was presented using a statistical z-test for the Elapsed time, Diversity, and RMSE as a performance indicator to maximize the energy efficiency and to minimize the exergy destruction with and without the rehear in Brayton system integrated to the ORC as bottoming cycle. The PSO optimization algorithm was evidenced by the best performance, and it is suggested in these applications based on the behavior of the swarming characteristics of the population.

Although both GA, RPS, and PSO are in the group of optimization algorithms are an important part of intelligent algorithms, they have some disadvantages that do not allow it to be applied to any optimization problem with an error ratio, diversity, and computational resource. To overcome these limitations, it is suggested to study the performance of algorithms based on the combination of both PSO and RPS with GA, in order to increase their overall performance. The combination of these optimization algorithms implies the development of an integrated algorithm with a high practical component, that works with a high degree of parallelism, where each particle is processed individually which makes possible the use of computers in parallel and the possibility of having more complex objective functions of thermo-economic and environmental character.

Declarations

Author contribution statement

Guillermo Eliecer Valencia: Conceived and designed the experiments; Performed the experiments; Analyzed and interpreted the data; Wrote the paper.

Jorge Duarte Forero: Conceived and designed the experiments; Performed the experiments; Analyzed and interpreted the data; Contributed reagents, materials, analysis tools or data.

Jhan Piero Rojas: Performed the experiments; Analyzed and interpreted the data; Contributed reagents, materials, analysis tools or data; Wrote the paper.

Funding statement

This research did not receive any specific grant from funding agencies in the public, commercial, or not-for-profit sectors.

Competing interest statement

The authors declare no conflict of interest.

Additional information

No additional information is available for this paper.

Acknowledgements

The authors thank the UNIVERSIDAD DEL ATLÁNTICO through the "PRIMERA CONVOCATORIA INTERNA PARA APOYO AL DESARROLLO DE TRABAJOS DE GRADO EN INVESTIGACIÓN FORMATIVA—NIVEL PREGRADO Y POSGRADO 2018", and UNIVERSIDAD FRANCISCO DE PAULA SANTANDER for their support on the development of this research.

References

[1] G. Valencia Ochoa, J. Nunez Alvarez, C. Acevedo, Research Evolution on Renewable Energies Resources from 2007 to 2017: a Comparative Study on Solar, Geothermal, Wind and Biomass Energy, 2019.

[2] G.V. Ochoa, J.N. Alvarez, M.V. Chamorro, Data set on wind speed, wind direction and wind probability distributions in Puerto Bolivar-Colombia, Data Br. 27 (2019) 104753.

[3] F.B. Budes, G.V. Ochoa, Y.C. Escorcia, An Economic Evaluation of Renewable and Conventional Electricity Generation Systems in a Shopping Center Using HOMER Pro®, 2017.

[4] D. Milani, M.T. Luu, R. McNaughton, A. Abbas, A comparative study of solar heliostat assisted supercritical CO_2 recompression Brayton cycles: dynamic modelling and control strategies, J. Supercrit. Fluids 120 (2017) 113–124.

[5] G. Valencia, A. Fontalvo, Y. Cardenas Escorcia, J. Duarte, C. Isaza-Roldan, Energy and exergy analysis of different exhaust waste heat recovery systems for natural gas engine based on ORC, Energies 12 (2019) 2378.

[6] G. Valencia Ochoa, C. Acevedo Peñaloza, J. Duarte Forero, Thermoeconomic optimization with PSO algorithm of waste heat recovery systems based on organic rankine cycle system for a natural gas engine, Energies 12 (21) (2019).
[7] G. Valencia, C. Peñaloza, J. Rojas, Thermoeconomic modelling and parametric study of a Simple ORC for the recovery of waste heat in a 2 MW gas engine under different working fluids, Appl. Sci. 9 (Oct. 2019) 4526.
[8] S. Quoilin, M. Van Den Broek, S. Declaye, P. Dewallef, V. Lemort, Techno-economic survey of organic rankine cycle (ORC) systems, Renew. Sustain. Energy Rev. 22 (2013) 168–186.
[9] J. Dyreby, S. Klein, G. Nellis, D. Reindl, Design considerations for supercritical carbon dioxide Brayton cycles with recompression, J. Eng. Gas Turbines Power 136 (10) (2014).
[10] P. Garg, P. Kumar, K. Srinivasan, Supercritical carbon dioxide Brayton cycle for concentrated solar power, J. Supercrit. Fluids 76 (2013) 54–60.
[11] J. Sarkar, Second law analysis of supercritical CO2 recompression Brayton cycle, Energy 34 (9) (2009) 1172–1178.
[12] M.S. Khan, M. Abid, H.M. Ali, K.P. Amber, M.A. Bashir, S. Javed, Comparative performance assessment of solar dish assisted s-CO2 Brayton cycle using nanofluids, Appl. Therm. Eng. 148 (2019) 295–306.
[13] L. Coco-Enríquez, J. Muñoz-Antón, J.M. Martínez-Val, Integration between direct steam generation in linear solar collectors and supercritical carbon dioxide Brayton power cycles, Int. J. Hydrogen Energy 40 (44) (2015) 15284–15300.
[14] J. Wang, Z. Sun, Y. Dai, S. Ma, Parametric optimization design for supercritical CO2 power cycle using genetic algorithm and artificial neural network, Appl. Energy 87 (4) (2010) 1317–1324.
[15] R. Chacartegui, J.M.M. De Escalona, D. Sánchez, B. Monje, T. Sánchez, Alternative cycles based on carbon dioxide for central receiver solar power plants, Appl. Therm. Eng. 31 (5) (2011) 872–879.
[16] S.J. Bae, Y. Ahn, J. Lee, J.I. Lee, Hybrid system of Supercritical Carbon Dioxide Brayton cycle and carbon dioxide rankine cycle combined fuel cell, in: In ASME Turbo Expo 2014: Turbine Technical Conference and Exposition, 2014.
[17] F. Alshammari, A. Pesyridis, A. Karvountzis-Kontakiotis, B. Franchetti, Y. Pesmazoglou, Experimental study of a small scale organic Rankine cycle waste heat recovery system for a heavy duty diesel engine with focus on the radial inflow turbine expander performance, Appl. Energy 215 (2018) 543–555.
[18] G. Valencia, J. Núñez, J. Duarte, Multiobjective optimization of a plate heat exchanger in a waste heat recovery organic rankine cycle system for natural gas engines, Entropy 21 (7) (2019).
[19] P. Song, M. Wei, L. Shi, S.N. Danish, C. Ma, A review of scroll expanders for organic rankine cycle systems, Appl. Therm. Eng. 75 (2015) 54–64.
[20] S. Quoilin, S. Declaye, B.F. Tchanche, V. Lemort, Thermo-economic optimization of waste heat recovery Organic Rankine Cycles, Appl. Therm. Eng. 31 (14–15) (2011) 2885–2893.
[21] G. Valencia, J. Duarte, C. Isaza-Roldan, Thermoeconomic analysis of different exhaust waste-heat recovery systems for natural gas engine based on ORC, Appl. Sci. 9 (19) (2019).
[22] O. Badr, P.W. O'Callaghan, S.D. Probert, Rankine-cycle systems for harnessing power from low-grade energy sources, Appl. Energy 36 (4) (1990) 263–292.
[23] A. Toffolo, A. Lazzaretto, G. Manente, M. Paci, A multi-criteria approach for the optimal selection of working fluid and design parameters in Organic Rankine Cycle systems, Appl. Energy 121 (2014) 219–232.
[24] V. Zare, A comparative exergoeconomic analysis of different ORC configurations for binary geothermal power plants, Energy Convers. Manag. 105 (2015) 127–138.
[25] K. Seshadri, Thermal design and optimization 21 (5) (1996).
[26] R. Smith, Chemical Process: Design and Integration, John Wiley & Sons, 2005.
[27] G. Towler, R. Sinnott, Chemical Engineering Design: Principles, Practice and Economics of Plant and Process Design, Elsevier, 2012.
[28] B. Franchetti, A. Pesiridis, I. Pesmazoglou, E. Sciubba, L. Tocci, Thermodynamic and Technical Criteria for the Optimal Selection of the Working Fluid in a Mini-ORC, 2016.
[29] S. Kelly, G. Tsatsaronis, T. Morosuk, Advanced exergetic analysis: approaches for splitting the exergy destruction into endogenous and exogenous parts, Energy 34 (3) (2009) 384–391.
[30] M. Yürüsoy, A. Keçebaş, Advanced exergo-environmental analyses and assessments of a real district heating system with geothermal energy, Appl. Therm. Eng. 113 (2017) 449–459.
[31] L. Barrios Guzman, Y. Cárdenas Escorcia, G. Valencia Ochoa, Análisis tendencial de las investigaciones de eficiencia energética en sistemas de refrigeración durante los años 2013 a 2017, Espacios 38 (54) (2017).
[32] H. Jouhara, M.A. Sayegh, Energy efficient thermal systems and processes, Therm. Sci. Eng. Prog. 7 (125–130) (2018) 1–5.
[33] R.V. Padilla, Y.C. Soo Too, R. Benito, W. Stein, Exergetic analysis of supercritical CO 2 Brayton cycles integrated with solar central receivers, Appl. Energy 148 (2015) 348–365.
[34] M. Aslam Siddiqi, B. Atakan, Alkanes as fluids in Rankine cycles in comparison to water and benzene, Proc. 24th Int. Conf. Effic. Cost Optim. Simul. Environ. Impact Energy Syst. ECOS 45 (1) (2011) 1544–1558.
[35] B.F. Tchanche, G. Lambrinos, A. Frangoudakis, G. Papadakis, Exergy analysis of micro-organic Rankine power cycles for a small scale solar driven reverse osmosis desalination system, Appl. Energy 87 (4) (2010) 1295–1306.
[36] S. Kiranyaz, Particle swarm optimization, Adapt. Learn. Optim. 15 (2014) 45–82.
[37] M. Lovay, G. Peretti, E. Romero, Aplicación del algoritmo Evolución Diferencial en un método de dimensionamiento para filtros bicuadráticos, in: 6th Argentine Symposium on Industrial Informatics, 46th Argentine Conference on Informatics, 2017, pp. 222–233.
[38] X.-S. Yang, 1 - optimization and metaheuristic algorithms in engineering, in: X.-S. Yang, A.H. Gandomi, S. Talatahari, A.H. Alavi (Eds.), Metaheuristics in Water, Geotechnical and Transport Engineering, Elsevier, Oxford, 2013, pp. 1–23.
[39] J. Kennedy, R. Eberhart, Particle swarm optimization, Int. Conf. Neural Networks 4 (1995) 1942–1948.
[40] Y. Feng, Y. Zhang, B. Li, J. Yang, Y. Shi, Comparison between regenerative organic Rankine cycle (RORC) and basic organic Rankine cycle (BORC) based on thermoeconomic multi-objective optimization considering exergy efficiency and levelized energy cost (LEC), Energy Convers. Manag. 96 (2015) 58–71.
[41] G. Valencia Ochoa, J. Cárdenas Gutierrez, J. Duarte Forero, Exergy, economic, and life-cycle assessment of ORC system for waste heat recovery in a natural gas internal combustion engine, Resources 9 (2020).
[42] H. Qi, et al., Application of multi-phase particle swarm optimization technique to inverse radiation problem, J. Quant. Spectrosc. Radiat. Transf. 109 (3) (2008) 476–493.
[43] G. Niu, B. Chen, J. Zeng, Repulsive particle swarm optimization based on new diversity, Chinese Contr. Decis. Conf. (2010) 815–819.